MedChemComm

CONCISE ARTICLE

View Article Online
View Journal | View Issue

Cite this: *Med. Chem. Commun.*, 2015, **6**, 1891

Identification of a novel NAMPT inhibitor by combinatorial click chemistry and chemical refinement†

S. Theeramunkong,‡[a] U. Galli,[a] A. A. Grolla,[a] A. Caldarelli,[a] C. Travelli,[a] A. Massarotti,[a] M. P. Troiani,[b] M. A. Alisi,[b] G. Orsomando,[c] A. A. Genazzani*[a] and G. C. Tron*[a]

Received 19th June 2015,
Accepted 3rd September 2015

DOI: 10.1039/c5md00261c

www.rsc.org/medchemcomm

The identification of compounds able to inhibit the NAD salvage pathway is experiencing a growing popularity as it has been proposed to be a novel target for antitumoral and anti-inflammatory drugs. In this manuscript, we used the copper-catalyzed [3+2] cycloaddition between azides and alkynes (click chemistry) to identify novel NAMPT inhibitors with a triazole-containing tail group. 720 compounds were synthesized in the first round, allowing the identification of 17 hit compounds. The second round of optimization brought about the discovery of compound **43** which displayed a cytotoxicity of 20 nM on neuroblastoma cancer cells and an inhibition of NAMPT of 114 nM.

Nicotinamide phosphoribosyltransferase (NAMPT) is a key, rate-limiting enzyme for the synthesis in cells of nicotinamide adenine dinucleotide (NAD) from nicotinamide.[1,2] Although other pathways that lead to NAD synthesis exist in mammals, NAMPT appears to be the enzyme in NAD metabolism most frequently up-regulated in metabolic, inflammatory and tumoral states.[3–6] Indeed, while NAD is relatively long-lived in cells as it is mainly used in redox reactions, a number of enzymes (*e.g.* sirtuins, PARPs) may consume it and active cells are in constant requirement of new NAD.[7–9] The identification in 2002 of **FK866** (Fig. 1), the first one-digit nanomolar NAMPT inhibitor,[10,11] followed shortly after by the resolution of the crystal structure of the enzyme bound to its inhibitor,[12] has opened the way for the medical exploitation of this biological target. After the disclosure of **FK866**, several groups both in industry and academia have searched and found small organic molecules able to inhibit NAMPT.[13,14] To date, only two compounds, **FK866** and **CHS828**, (Fig. 1) as its water soluble pro-drug teglarinad,[15] have reached clinical trials in cancer. *In vivo* studies have anyway shown low bioavailability for **FK866** (ref. 16) and, in addition, both **CHS828** and **FK866** give rise to thrombocytopenia and various gastrointestinal symptoms (phase I clinical trials).[16,17] A recent pre-clinical study also suggests that the retinal toxicity[18] may be relevant for most NAMPT inhibitors as it appears to be an on-target side effect. Furthermore, metabolism may also be an issue.[19] For this reason, the search and development of safer NAMPT inhibitors is still a topic of interest. All the NAMPT inhibitors reported to date, which were recently reviewed,[13,14] share a common pharmacophoric working model: a *meta* or *para*

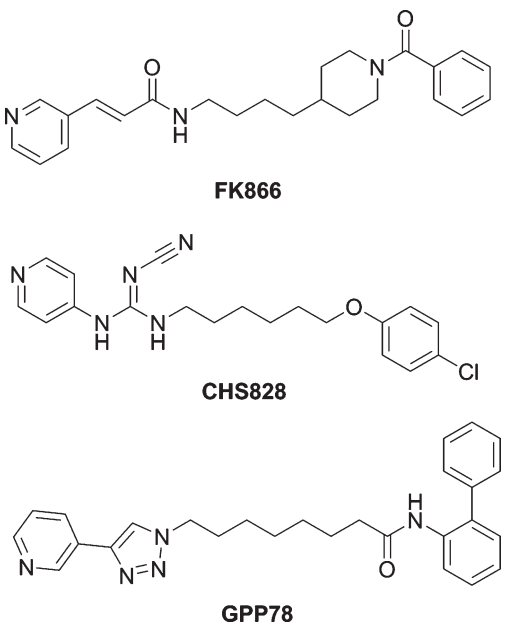

Fig. 1 Structures of **FK866**, **CHS828**, and **GPP78**.

[a] *Dipartimento di Scienze del Farmaco, Università degli Studi del Piemonte Orientale "A. Avogadro", Largo Donegani 2, 28100 Novara, Italy. E-mail: armando.genazzani@uniupo.it, giancesare.tron@uniupo.it; Fax: +39 0321375821; Tel: +39 0321375827*

[b] *R&D, Angelini Research Center, Piazzale della Stazione, 00040 S. Palomba-Pomezia, Italy*

[c] *Department of Clinical Sciences (DISCO), Section of Biochemistry, Polytechnic University of Marche, Via Ranieri 67, Ancona 60131, Italy*

† Electronic supplementary information (ESI) available: Materials and methods. See DOI: 10.1039/c5md00261c

‡ Current address: Faculty of Pharmacy, Thammasat University (Rangsit Campus), 99 Phahon Yothin Rd., Khlong Luang, Pathum Thani, 12120, Thailand.

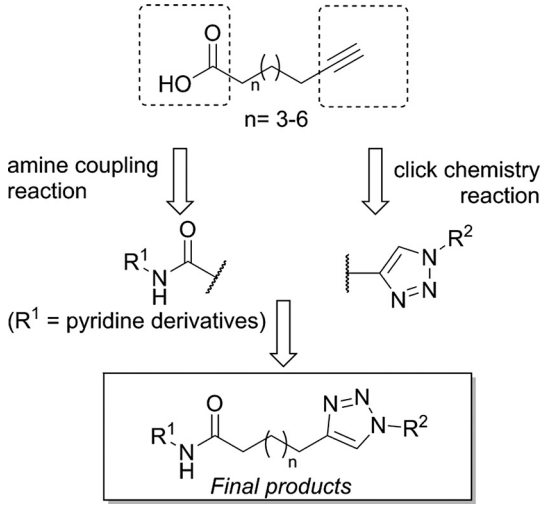

Fig. 2 The three main parts of the starting compounds: an alkyne, a methylene chain and a carboxylic acid moiety.

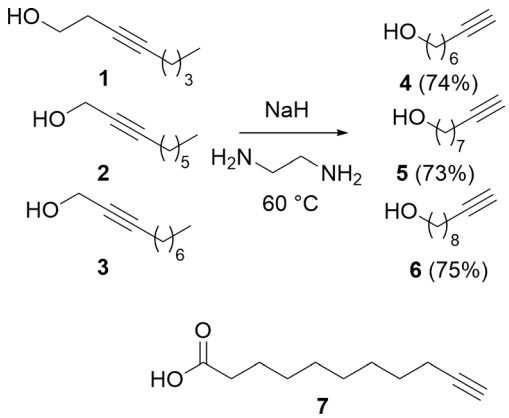

Scheme 1 Acetylene zipper reaction of alcohol derivatives with internal alkynes and the structure of 10-undecynoic acid (7).

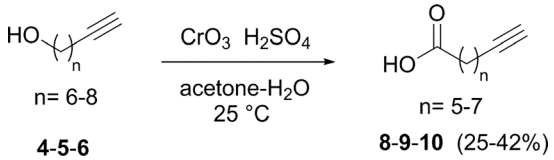

Scheme 2 Oxidation of alcohols by the Jones reaction.

substituted pyridine or an heterocycle containing pyridine as a cap group, a connecting unit with a hydrogen bond acceptor, an alkyl chain linker and a hydrophobic tail group able to interact with the hydrophobic amino acids at the rim of the enzyme. In 2010, our group, using click chemistry, discovered a one-digit nanomolar NAMPT inhibitor (EC_{50} for cytotoxicity *in vitro* of 3.8 ± 0.3 nM and IC_{50} for NAD depletion of 3.0 ± 0.4 nM on the SH-SY5Y cell line),[20] named **GPP78** (Fig. 1), exploiting the bioisosterism between the amide of **FK866** and the 1,2,3-triazole ring.[21]

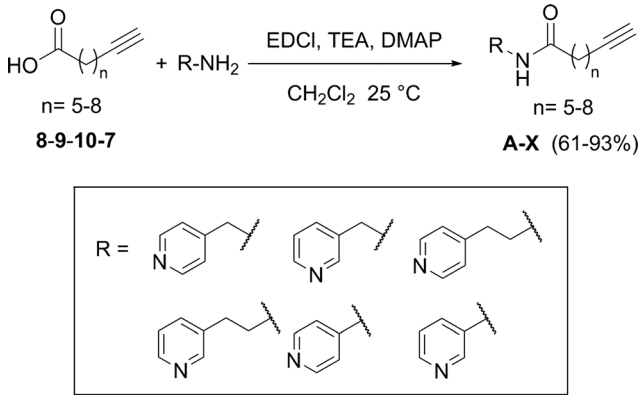

Scheme 3 Coupling reaction between carboxylic acids and amines to obtain amide compounds.

With the goal of identifying novel NAMPT inhibitors, always using click chemistry and exploiting a combinatorial approach, we investigated the possibility of identifying novel tail groups. To accomplish this task, a set of ω-alkyl carboxylic acids were used as functional building blocks. These structures contain three main parts: an alkyne, a methylene chain and an acid moiety. The alkyne part undergoes click chemistry reaction with different azide derivatives to create different tail groups. The linker, five to eight methylene units long, allows the cap group to enter the catalytic tunnel, and finally the carboxylic acid can be coupled with different amino pyridines forming the cap group (Fig. 2).

The ω-alkyl carboxylic acids (**8–10**) were prepared starting from the commercially available alcohols containing an internal alkyne (**1–3**) using the acetylene zipper reaction,[22] while for the alkyl chain with eight methylene groups, 10-undecynoic acid (**7**) was commercially available (Scheme 1). The alcoholic function of **4–6** was then oxidized to carboxylic acid under Jones conditions (Scheme 2). The yields of these reactions were modest (25–42%) as it was not possible to suppress the side reaction leading to the esterification of the carboxylic product with the alcohol.

The 4 carboxylic acids were then coupled with 6 commercial amines containing a pyridine ring to obtain 24 different amides (Scheme 3). The structures of amides (**A–X**) are shown in Fig. 3.

The resulting terminal alkyne-amides and 30 in-house azides (**11–40**, Fig. 4) were used for the copper(I) catalyzed [3+2] cycloaddition to give 720 triazole products (Scheme 4).

All the compounds were subjected to MS analysis to verify the presence of the desired triazoles and used as such without purification after evaporation of the solvent. Given the elevated number of compounds, the screening procedure did not evaluate the purity by LC-MS but only the presence of the desired compound. The 720 crude compounds were then screened for cytotoxicity *via* the MTT method using SH-SY5Y neuroblastoma cancer cells at a fixed concentration (10 μM). This cell line was chosen as we have gathered considerable

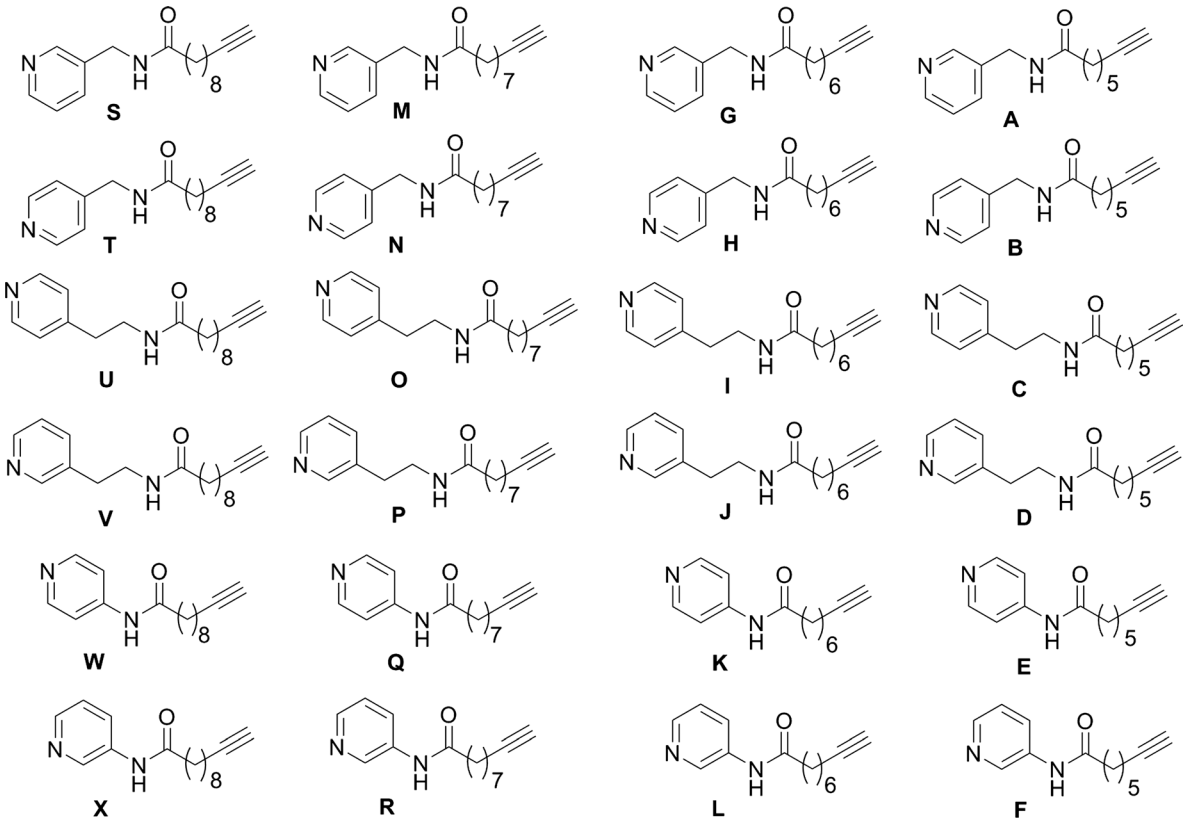

Fig. 3 Structures of the amides (**A**–**X**) synthesized.

evidence that it is sensitive to NAMPT inhibitors.[23] While an enzyme screening using recombinant NAMPT could also have been considered to highlight possible hits, we preferred this biological surrogate assay as important discrepancies have been described between cellular and enzymatic activities and have been attributed to the ability of some inhibitors to form phosphoribosyl adducts with the enzyme that can also lead to cellular accumulation.[24] The enzymatic assay, unlike the cytotoxicity assay, does not discriminate between inhibitors that can or cannot forms adducts.[24] It should also be noted that the enzyme assay is more sensitive to possible contaminants and compounds would have needed to undergo purification; moreover the biological assay is extremely more economical. Data for this screening is presented in the ESI (Table S1†). As trace amounts of copper salts could be present in the precipitated products, we also evaluated the cytotoxicity of these salts in our cancer cell line. Neither copper(II) sulphate nor copper(I) iodide displayed cytotoxic effects up to 10 μM. Similar data on the lack of confounding effect of copper salts had been published previously.[25]

The first screening yielded seventeen compounds that were able to reduce viability by >60% compared to the control: **A12**, **C13**, **D12**, **G12**, **M14**, **M28**, **O14**, **P14**, **P34**, **Q12**, **Q39**, **Q40**, **R12**, **S31**, **S39**, **W31**, and **W39** (Fig. S1†). These compounds were then subject to chromatographic purification and tested at increasingly lower concentrations.

The cytotoxic effects of these seventeen purified compounds are reported in Table 1. Only 8 compounds retained activity once purified and, of these, two displayed considerable activity also at 1 μM. The presence of false positives in the initial screening is not surprising and might be due to inaccuracies in the biological assay as well as to the presence of contaminants in the crude precipitate obtained. A full concentration–response curve of these two compounds (the biphenyl-triazoles **A12** and **D12**, Fig. 5) was obtained and the EC_{50}s for cytotoxicity were 456.2 ± 3.2 nM and 680.5 ± 30 nM, respectively. As cytotoxicity is not necessarily a surrogate marker for NAMPT inhibition, we also obtained a concentration–response curve for enzyme inhibition *in vitro*. **A12** displayed an IC_{50} of 267 ± 94 nM and **D12** displayed an IC_{50} of 170 ± 21 nM. In the assay conditions used, **FK866** yielded an EC_{50} for enzyme inhibition of 61 ± 7 nM.

Molecular modeling studies were then performed to investigate the potential pose of **A12** and **D12** in the **FK866** binding site of NAMPT (PDB id: 2GVJ). Docking studies were carried out using the software OMEGA2 (ref. 26 and 27) and FRED,[28,29] showing that the two structures lay with the same orientation as **FK866**. The structural water molecule appears to be irrelevant to reproduce the **FK866** crystal pose, therefore it was not considered in the docking simulations. The pyridine ring was stabilized in the active site by a π–π stacking interaction with Phe193 and Tyr18′.

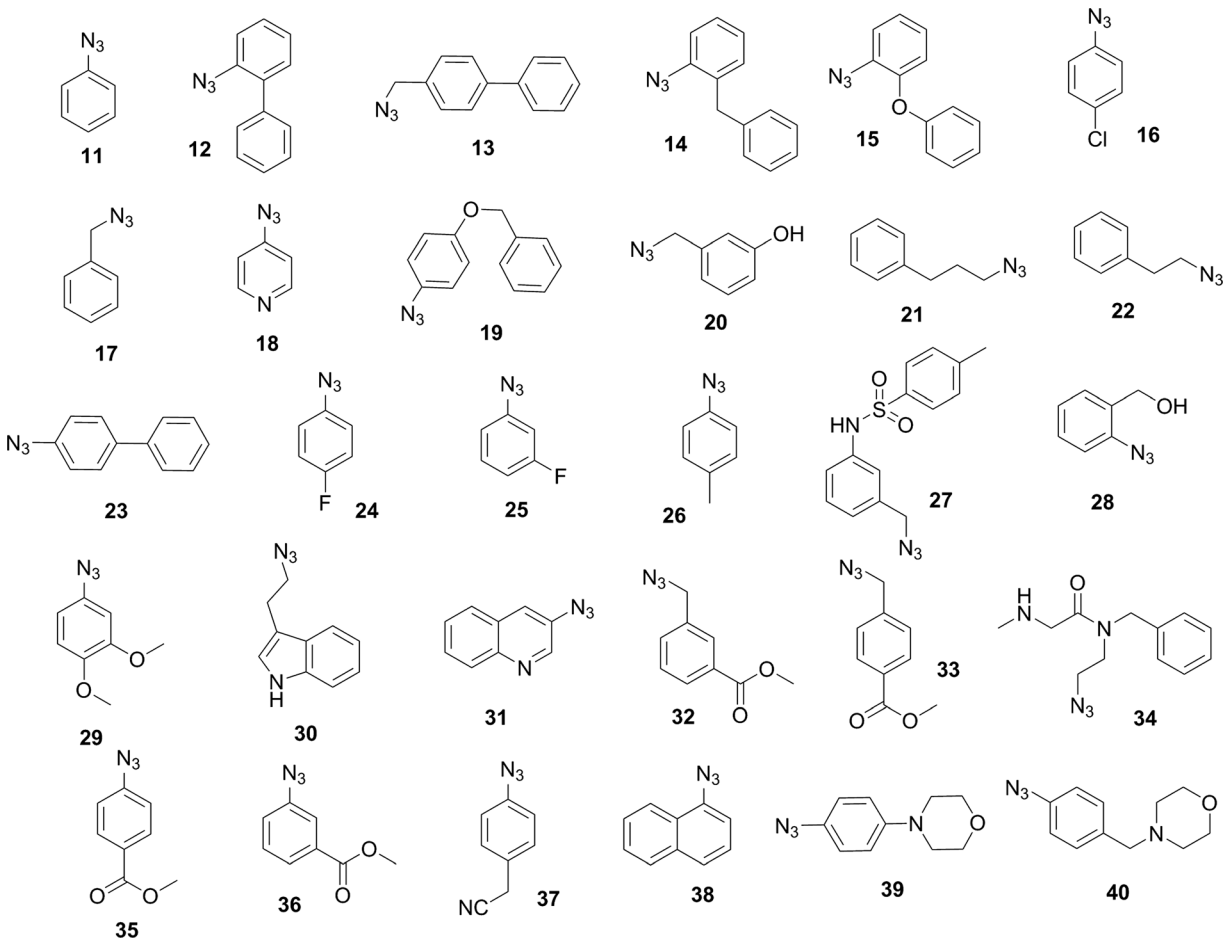

Fig. 4 Structures of in-house azides (**11**–**40**).

The carbonyl moiety was positioned in the binding cavity near Ser275, accepting a hydrogen bond for both compounds, while only the amide nitrogen of **A12** was able to form an H-bond interaction with Val242. The biphenyl group occupies the same cavity around Ala379 and Lys189 in the case of compound **A12**, while it has a different orientation involving a π–π stacking interaction with Tyr188 in the case of **D12** (Fig. 6).

This molecular modeling study suggests that both **A12** and **D12** have longer H-bonding interactions compared to **FK866**. For this reason, in an attempt to improve the potency of the compounds, we decided to reverse the amide group (compounds **41** and **42**, Fig. 7) as it appears to give a better H-bonding interaction.

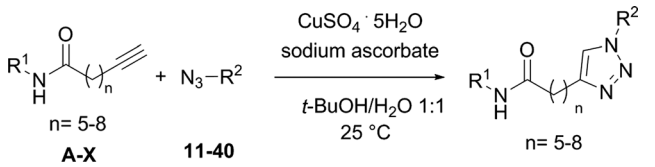

Scheme 4 [3+2] cycloaddition between alkyne and azide to obtain 1,4-disubstituted triazoles.

In addition, we synthesized the analogue with an *E*-double bond between the amide and the pyridine group (compound **43**),

Table 1 Viability of SH-SY5Y cells treated with the purified 17 triazole products and enzyme inhibition activity. Data represent %cell viability in mean ± SD of at least 4 determinations and %inhibition in mean ± SD of at least 3 determinations

Comp.	%Cell viability (mean ± SD) 10 μM	1 μM	EC_{50} (nM) for cell viability	IC_{50} (nM) for NAMPT activity
A12	12.5 ± 0.5	13.4 ± 0.5	456 ± 3.2	267 ± 94
C13	100 ± 10			
D12	25 ± 1	29.2 ± 1.1	680 ± 30	170 ± 21
G12	47 ± 6	98 ± 7		
M14	94 ± 3			
M28	96 ± 13			
O14	99 ± 13			
P14	101 ± 13			
P34	109 ± 9			
Q12	32 ± 1	82 ± 3		
Q39	103 ± 10			
Q40	125 ± 18			
R12	111 ± 6			
S31	29 ± 1	102 ± 8		
S39	74 ± 3	100 ± 2		
W31	53 ± 3	104 ± 6		
W39	28 ± 1	93 ± 2		

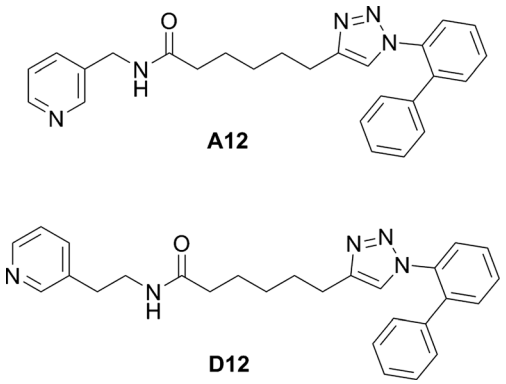

Fig. 5 Structures compounds able to display considerable activity at 1 μM.

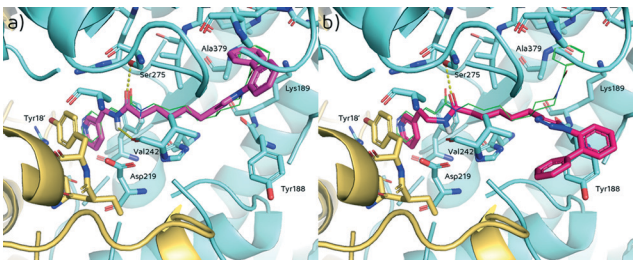

Fig. 6 Complex structure of hNAMPT enzyme and docked ligands (I). Docking pose of **A12** (a) and **D12** (b) are shown in pink sticks. **FK866** is superimposed as a green wire model. The backbone of hNAMPT is shown as a ribbon representation (yellow and cyan). The amino acids of hNAMPT within 4.0 Å from **FK866** are shown as wire models. Hydrogen bonds (distance <3 Å) are shown as dotted yellow lines.

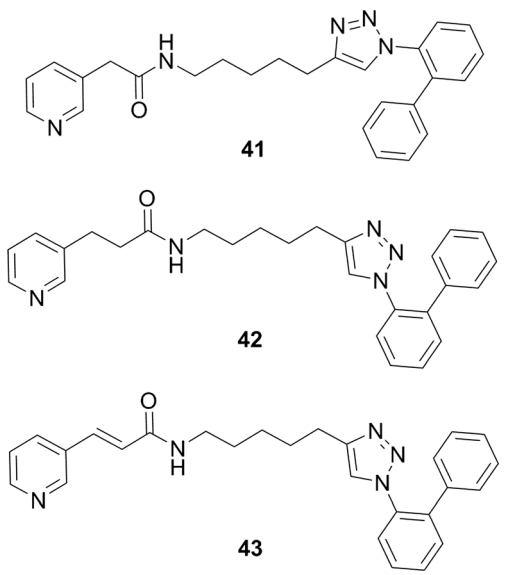

Fig. 7 Structure of compounds **41**, **42** and **43**.

mimicking the structure of **FK866**; as with our molecular modeling studies we found that the interaction pattern of **43** was similar to that of **FK866** (Fig. 8).

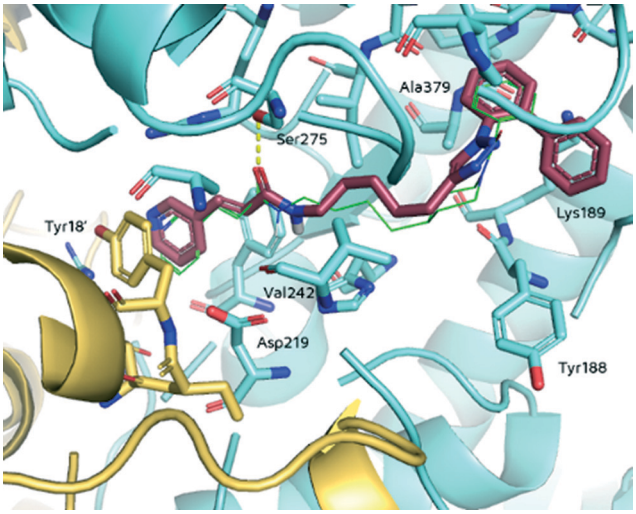

Fig. 8 Complex structure of hNAMPT enzyme and docked ligands (II). The docking pose of **43** is shown in brown sticks. **FK866** pose is superimposed as a green wire model. The backbone of hNAMPT is shown as a ribbon representation (yellow and cyan). The amino acids of hNAMPT within 4.0 Å from **FK866** are shown as wire models. Hydrogen bonds (distance <3 Å) are shown as dotted yellow lines.

To prepare these three compounds, we started from commercially available 6-heptynenitrile (**44**) which was coupled with azide **12** *via* click reaction. The resulting nitrile **45** was reduced to amine **46** using $LiAlH_4$ and coupled with three different carboxylic acids (**47**, **48**, and **49**) to obtain the desired amide products **41**–**43** (Scheme 5).

The cytotoxic results are reported in Table 2. Compounds **41** and **42** were inactive at 100 nM while compound **43** was the most active with an IC_{50} of 20.0 ± 0.7 nM on neuroblastoma cells. The *in vitro* enzyme assay supported the activity of this compound, with an IC_{50} of approx. 114 ± 12 nM in the enzymatic assay for NAMPT activity. **FK866**, in our assay, inhibited recombinant NAMPT with an IC_{50} of 61 ± 7 nM.

Last, in order to confirm the rank order of potency of these compounds, we evaluated cellular NAD depletion in SH-SY5Y cells treated with increasing concentrations of **FK866**, **A12**, **D12**, and **43** for 16 hours. The rank order of potency was maintained with respect to the other assays performed, with **A12** and **D12** significantly less potent (IC_{50}s of 1.1 ± 0.3 nM and 7.6 + 1.6 nM, respectively) compared to **FK866** and **43** (30.1 ± 5.9 pM and 50.9 ± 21.5 pM, respectively) (Fig. 9).

Conclusions

In conclusion, in the present study we employed click chemistry to synthesize 720 new compounds starting from simple building blocks. We screened them for cytotoxicity and NAMPT inhibition and then attempted to optimize them after obtaining the initial biological data. This strategy led to a compound with an EC_{50} for cytotoxicity of approx. 20 nM and an IC_{50} for enzyme inhibition of approx. 100 nM that displayed a 2-biphenyl-1,2,3-triazole as a novel tail group.

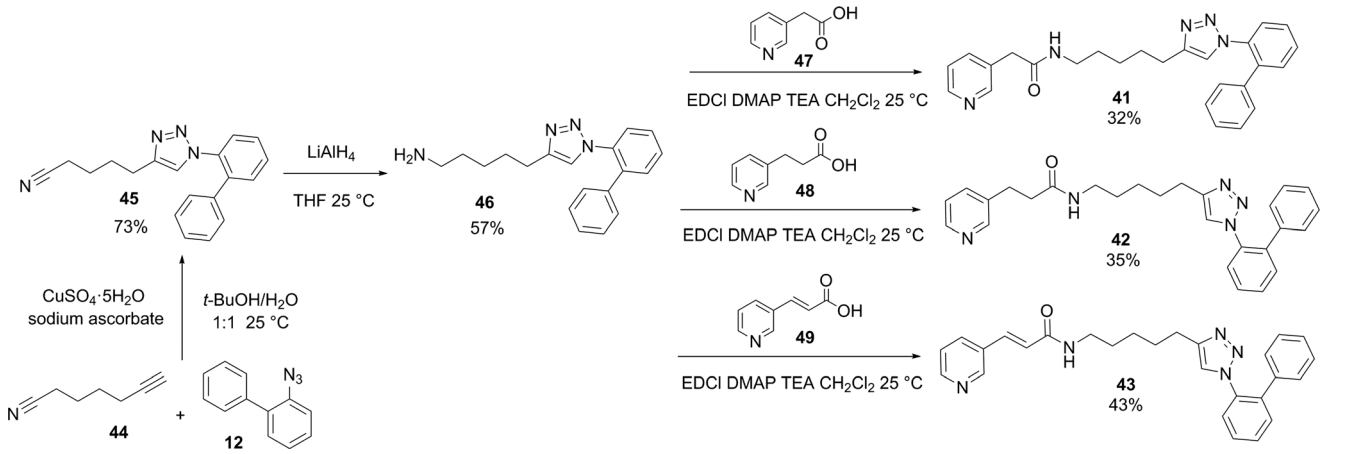

Scheme 5 Synthesis of three modified compounds (**41**–**43**).

Table 2 Viability of SH-SY5Y cells treated with **41**, **42** and **43** at 1 μM and 100 nM for 48 hours and enzyme inhibition of **43**. Data represent mean ± SD of at least 4 determinations

Comp.	%Cell viability (mean ± SD) 1 μM	100 nM	EC_{50} (nM) for cell viability	IC_{50} (nM) for NAMPT activity
41	99 ± 1	106 ± 2		
42	54 ± 1	112 ± 1		
43	32 ± 1	49 ± 3	20 ± 0.7	114 ± 12
FK866			3.2 ± 0.4	61 ± 7

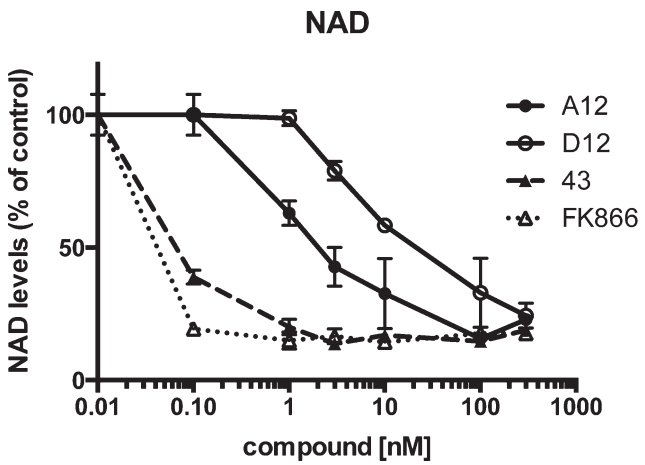

Fig. 9 Effect of NAMPT inhibitors on cellular NAD levels. Cells were treated with the indicated compounds for 16 hours. n = 6 from two separate experiments. IC_{50}s are indicated in the main text.

Acknowledgements

Financial support from AIRC to AAG (IG10509) and to CT (Leonino Fontana e Maria Lionello Fellowship, 14832), as well as financial support from the Fondazione San Paolo to AAG (oncoNAMPT) and the Italian Ministry of Education to GCT (PRIN-2010W7YRLZ_002), is gratefully acknowledged. This work was also made possible by a research contract grant between the Department of Pharmaceutical Sciences and Angelini Research Center.

Notes and references

1 G. Magni, A. Amici, M. Emanuelli, N. Raffaelli and S. Ruggieri, *Adv. Enzymol. Relat. Areas Mol. Biol.*, 1999, **73**, 135–182, xi.
2 A. Chiarugi, C. Dolle, R. Felici and M. Ziegler, *Nat. Rev. Cancer*, 2012, **12**, 741–752.
3 A. Garten, S. Petzold, A. Korner, S. Imai and W. Kiess, *Trends Endocrinol. Metab.*, 2009, **20**, 130–138.
4 S. Imai, *Curr. Pharm. Des.*, 2009, **15**, 20–28.
5 M. Galli, F. Van Gool, A. Rongvaux, F. Andris and O. Leo, *Cancer Res.*, 2010, **70**, 8–11.
6 L. Q. Zhang, D. P. Heruth and S. Q. Ye, *J. Bioanal. Biomed.*, 2011, **3**, 13–25.
7 M. Ziegler, *Eur. J. Biochem.*, 2000, **267**, 1550–1564.
8 H. C. Lee, *Annu. Rev. Pharmacol. Toxicol.*, 2001, **41**, 317–345.
9 D. Corda and M. Di Girolamo, *EMBO J.*, 2003, **22**, 1953–1958.
10 K. Wosikowski, K. Mattern, I. Schemainda, M. Hasmann, B. Rattel and R. Loser, *Cancer Res.*, 2002, **62**, 1057–1062.
11 M. Hasmann and I. Schemainda, *Cancer Res.*, 2003, **63**, 7436–7442.
12 J. A. Khan, X. Tao and L. Tong, *Nat. Struct. Mol. Biol.*, 2006, **13**, 582–588.
13 U. Galli, C. Travelli, A. Massarotti, G. Fakhfouri, R. Rahimian, G. C. Tron and A. A. Genazzani, *J. Med. Chem.*, 2013, **56**, 6279–6296.
14 D. Sampath, T. S. Zabka, D. L. Misner, T. O'Brien and P. S. Dragovich, *Pharmacol. Ther.*, 2015, **151**, 16–31.
15 P. Beauparlant, D. Bedard, C. Bernier, H. Chan, K. Gilbert, D. Goulet, M. O. Gratton, M. Lavoie, A. Roulston, E. Turcotte and M. Watson, *Anti-Cancer Drugs*, 2009, **20**, 346–354.
16 K. Holen, L. B. Saltz, E. Hollywood, K. Burk and A. R. Hanauske, *Invest. New Drugs*, 2008, **26**, 45–51.
17 A. von Heideman, A. Berglund, R. Larsson and P. Nygren, *Cancer Chemother. Pharmacol.*, 2010, **65**, 1165–1172.

18 T. S. Zabka, J. Singh, P. Dhawan, B. M. Liederer, J. Oeh, M. A. Kauss, Y. Xiao, M. Zak, T. Lin, B. McCray, N. La, T. Nguyen, J. Beyer, C. Farman, H. Uppal, P. S. Dragovich, T. O'Brien, D. Sampath and D. L. Misner, *Toxicol. Sci.*, 2015, **144**, 163–172.
19 M. Zak, B. M. Liederer, D. Sampath, P. W. Yuen, K. W. Bair, T. Baumeister, A. J. Buckmelter, K. H. Clodfelter, E. Cheng, L. Crocker, B. Fu, B. Han, G. Li, Y. C. Ho, J. Lin, X. Liu, J. Ly, T. O'Brien, D. J. Reynolds, N. Skelton, C. C. Smith, S. Tay, W. Wang, Z. Wang, Y. Xiao, L. Zhang, G. Zhao, X. Zheng and P. S. Dragovich, *Bioorg. Med. Chem. Lett.*, 2015, **25**, 529–541.
20 G. Colombano, C. Travelli, U. Galli, A. Caldarelli, M. G. Chini, P. L. Canonico, G. Sorba, G. Bifulco, G. C. Tron and A. A. Genazzani, *J. Med. Chem.*, 2010, **53**, 616–623.
21 A. Massarotti, S. Aprile, V. Mercalli, E. Del Grosso, G. Grosa, G. Sorba and G. C. Tron, *ChemMedChem*, 2014, **9**, 2497–2508.
22 S. E. Denmark and S.-M. Yang, *Tetrahedron*, 2004, **60**, 9695–9708.
23 U. Galli, E. Ercolano, L. Carraro, C. R. Blasi Roman, G. Sorba, P. L. Canonico, A. A. Genazzani, G. C. Tron and R. A. Billington, *ChemMedChem*, 2008, **3**, 771–779.
24 A. Oh, Y. C. Ho, M. Zak, Y. Liu, X. Chen, P. W. Yuen, X. Zheng, Y. Liu, P. S. Dragovich and W. Wang, *ChemBioChem*, 2014, **15**, 1121–1130.
25 T. Pirali, F. Pagliai, C. Mercurio, R. Boggio, P. L. Canonico, G. Sorba, G. C. Tron and A. A. Genazzani, *J. Comb. Chem.*, 2008, **10**, 624–627.
26 *OMEGA, version 2.4.6*, OpenEye Scientific Software, Santa Fe, NM, http://www.eyesopen.com.
27 P. C. D. Hawkins, A. G. Skillman, G. L. Warren, B. A. Ellingson and M. T. Stahl, *J. Chem. Inf. Model.*, 2010, **50**, 572–584.
28 *FRED, version 3.0.0*, OpenEye Scientific Software, Santa Fe, NM, http://www.eyesopen.com.
29 M. McGann, *J. Chem. Inf. Model.*, 2011, **51**, 578–596.